

On User-Level CSMA for Multi-Channel Wireless Networks

Thomas Bonald*and Mathieu Feuillet†

October 26, 2018

Abstract

We consider a multi-channel wireless network with *user-level* CSMA, which consists in running one instance of the CSMA algorithm per active user at each MAC interface. Specifically, each such instance attempts to access a randomly chosen radio channel after some random time and transmits a packet of the corresponding user if the channel is sensed idle. We prove that, unlike the standard CSMA algorithm, this simple distributed access scheme is optimal in the sense that the network is stable for all traffic intensities in the capacity region of the network. Simulations show that capacity (in terms of maximum sustainable traffic) increases by a factor ranging from 1.5 to 2.5 compared to the standard CSMA algorithm, depending on the network topology and the number of available radio channels.

1 Introduction

The CSMA (Carrier Sense Multiple Access) algorithm is a key component of IEEE 802.11 networks. While it proves successful in sharing the radio channel of a single access point, its efficiency is questionable in more involved environments with multiple interfering access points. First, the phenomenon of head-of-line blocking prevents an access point from taking advantage of spatial reuse, whereby users with favorable transmission conditions are opportunistically scheduled [14, 4]. Next, the phenomenon of hidden nodes requires the use of the standard RTS/CTS (Request To Send/Clear To Send) signals before any transmission so as to ensure an efficient utilization of the radio channel [37]. These mechanisms in turn may cause the starvation of some access points whose activity conflicts with that of surrounding access points, as illustrated by Fig. 1. As a result, the CSMA algorithm is not able to fully utilize network capacity, a statement that will be made more precise later in the paper.

We propose a slight modification of the CSMA algorithm that accounts for the congestion suffered by each node. Specifically, each MAC (Medium Access Control) interface maintains a separate queue per active user and runs one CSMA instance per queue. That queue whose backoff timer expires first will access the channel, provided the latter is sensed idle. This simple mechanism, referred to as *user-level* CSMA, enables spatial reuse and gives preferential access to those nodes that suffer from congestion. We shall see that it actually guarantees the optimal utilization of the radio channel. Specifically, it stabilizes the network, in the sense that the number of active users reaches a finite steady state, whenever possible.

Clearly, the efficiency of the proposed CSMA algorithm comes from the fact that the attempt rate of each node in accessing the channel increases with the number of active users at this node. As explained in the next section, the fact that such a simple algorithm suffices to guarantee the *optimal* utilization of the radio channel is far from obvious, however. It solves a tough issue in the field of optimal distributed scheduling in a very general setting where the interactions

*T. Bonald is with the Department of Computer Science and Networking, Telecom ParisTech, Paris, France. Email: thomas.bonald@telecom-paristech.fr

†M. Feuillet is with INRIA, Paris-Rocquencourt, France. Email: mathieu.feUILLET@inria.fr

between interfering wireless links are represented by an arbitrary conflict graph. Moreover, our result applies to multi-channel networks, each user selecting a radio channel at random, and in the presence of multiple transmitters, some nodes being able to send data over several radio channels at the same time. We believe that such networks will be key in the future, due to the expected growth of unlicensed radio spectrum, that will likely be accessed in a fully distributed, opportunistic way.

It is worth mentioning that the proposed user-level CSMA also guarantees *fairness* in channel utilization. It is well-known that, under standard CSMA, downstream flows (from the access point to the users) are penalized compared to upstream flows (from the users to the access point), see [9] for instance. This is because, when n users are connected to the same access point, there are n upstream CSMA instances competing with only one downstream CSMA instance. Under user-level CSMA, there is one instance of CSMA per user in each direction, upstream and downstream, so that each user packet stream gets the same bandwidth share. In the above example with a single access point, the whole system can actually be viewed as a unique, evenly shared wireless link. In general, the system behaves *as if* each user packet stream constitutes an independent link, whose throughput depends on the whole set of active links and their mutual interference.

The rest of the paper is organized as follows. Related work is presented in the next section. We then present the model and analyze its stability behavior under standard and user-level CSMA, respectively. The throughput performance of both algorithms are compared by simulation in Section 6. Section 7 concludes the paper.

2 Related Work

The problem of optimal bandwidth sharing in wireless networks has first been tackled by Tassiulas and Ephremides, who showed in [36] that the so-called *maximal weight* scheduling policy, which activates a set of links that maximizes the total backlog of active links, stabilizes any network whenever possible. A number of distributed implementations of this policy have then been proposed, all relying on some message passing protocol between nodes, see e.g. [24, 32]. Simple heuristics based on greedy algorithms that require limited or no message passing have also been studied, most selecting schedules of *maximal size* (in terms of number of links) instead of maximal weight [7, 10, 15, 19, 28]. It has been proven in [40, 6] that these algorithms stabilize the network for at least a fraction of the maximum capacity, this fraction depending on the topology. The actual stability condition achieved by these algorithms is an open question, except under some specific assumptions like coupled arrival processes [6]. It turns out that the standard CSMA algorithm belongs to this class of greedy algorithms in the limiting regime of infinite attempt rates. We provide two examples of networks, with a single channel and multiple channels, respectively, for which it is provably suboptimal in this limiting regime.

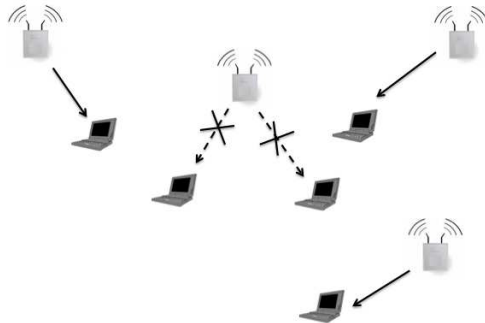


Figure 1: Starvation of an access point due to interference.

A new approach to optimal scheduling has recently been proposed by Jiang and Walrand, who introduced in [12] a distributed CSMA algorithm where at each link, the attempt rate is adapted to the arrival rate and service rate so as to meet the demand. This approach is based on a time-scale separation assumption whereby the activity states of the links, which depend on the CSMA algorithm, evolve much faster than the attempt rates of the links. In practice, the algorithm used for adapting the attempt rates must be carefully designed in order to guarantee convergence and optimality [12, 29, 30, 11]. Similar problems arise for those adaptive CSMA algorithms where the attempt rates are functions of the *queue lengths* instead of some slowly varying estimates of the arrival rates and service rates: the algorithm converges only for some specific choices of these functions [26, 31].

In all these papers, optimality is defined either in terms of stability, assuming exogenous random packets arrivals at each link, or in terms of utility maximization, cf. [12, 29]. The flow-level dynamics are not considered, whereas they are key to understanding network performance [22]. In particular, it can be argued that the very notion of *congestion* should be defined at the flow level, taking into account the evolution of the number of active users [1]. In a recent paper, van de Ven, Borst and Shneer have shown that the maximal weight scheduling policy, which is known to stabilize the network at packet level, may be unable to stabilize the network at flow level, for a single access point with time-varying downlink channels [39]. Some scheduling algorithms that are optimal *at flow level* have been proposed in this context, see [39, 20] for instance. The main contribution of the present paper is to provide a distributed algorithm that is optimal at flow level for *any* network of conflicting wireless links.

With this objective in mind, it is very natural to think of user-level CSMA. The fact that it suffices to run an instance of the CSMA algorithm per active user at each MAC interface is far from obvious, however. Some networks may for instance be unstable under usual traffic conditions whereas the total throughput of all links is maximized at any time [5]. It turns out that the fairness imposed by the proposed user-level CSMA algorithm is indeed sufficient to achieve stability.

Specifically, the user-level CSMA algorithm selects each feasible schedule in proportion to its *weight*, where the weight of a schedule is the *product* of the number of active users on the corresponding links. For a large number of active users, the selected schedules are close to the corresponding *maximal weight* schedule (with product weights instead of additive weights), a policy that turns out to be optimal. We note that a similar property is used by Ni, Bo and Srikant in [26] for proving the stability of queue-length based CSMA at packet level. The constraints imposed by the packet level, like the above mentioned problem of time-scale separation that restricts the set of eligible weight functions, make their algorithm very different from ours, however. Our model is purely asynchronous and stateless; moreover, the time-scale separation assumption naturally follows from the fact that the attempt rates evolve at the flow time-scale, which is typically much slower than the packet time-scale. The simulation results of Section 6 confirm this intuition.

A preliminary version of this work focussed on networks with a single channel [3]. Surprisingly, little attention has been paid to multi-channel networks. Existing algorithms are either suboptimal [38, 35], centralized [25, 16, 21] or focus on utility maximization, in the absence of flow-level dynamics [29]. To our knowledge, user-level CSMA is the first distributed algorithm that is provably optimal in terms of stability in the general case of multiple channels and multiple transmitters per link.

3 Model

3.1 Wireless network

The network consists of K links and J orthogonal radio channels. Each link is an ordered source-destination pair. The source of link k is equipped with n_k transmitters and thus can use up to n_k distinct radio channels simultaneously. Each channel j is associated with some *conflict graph* $G_j = (V_j, E_j)$, where V_j is the set of vertices, each representing a link that can use channel j , and E_j is the set of edges, each representing a conflict. Two links $k, l \in V_j$ can be simultaneously

active on channel j if and only if they do not conflict, that is if $(k, l) \notin E_j$. The J conflict graphs are typically the same but could differ due to different radio propagation environments on the J channels, or different transmission capabilities of the K sources (some sources may access only a subset of the J channels).

We refer to a *feasible schedule* as any sets of links $S_1 \subset V_1, \dots, S_J \subset V_J$ such that, on each channel j , the links in set S_j do not conflict with each other, and the total number of channels used by link k ,

$$y_k = \sum_{j=1}^J \mathbb{1}(k \in S_j),$$

does not exceed n_k . Let I be the number of distinct feasible schedules. For each schedule i , we denote by S_{ij} the set of active links on channel j and by

$$y_{ik} = \sum_{j=1}^J \mathbb{1}(k \in S_{ij})$$

the number of active channels on link k . By convention, schedule 1 corresponds to that schedule where all nodes are idle, that is $S_{1j} = \emptyset$ for all $j = 1, \dots, J$.

Consider for instance the network of $K = 3$ links and $J = 1$ channel depicted by Fig.2. Two links conflict if and only if the distance between the source or destination of one link and the source or destination of the other link is less than some given threshold, that typically corresponds to the transmission range of the RTS/CTS signals. The conflict graph is linear and there are $I = 5$ feasible schedules, corresponding to the sets of active links $\emptyset, \{1\}, \{2\}, \{3\}, \{1, 3\}$.

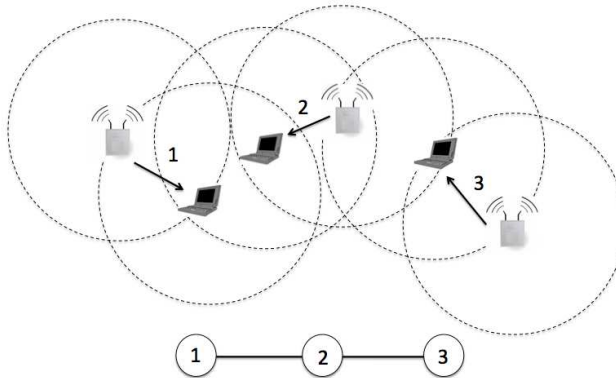


Figure 2: A 3-link network and its conflict graph.

Note that links may also correspond to *groups* of source-destination pairs that have the same conflicts. For instance, the network of three access points depicted by Fig. 3 is associated with $K = 7$ “links” corresponding to the different sets of access points that are involved in the transmission of a packet from an access point to some user in its transmission range. Each of these sets contains the transmitting access point and the potentially conflicting access points, that typically receive the CTS message from the destination and thus conflict with the transmission. Note that the identity of the transmitting access point in this set does not matter. Links 1,2,3 correspond to source-destination pairs that do not conflict with any other access point, links 4,5,6 correspond to source-destination pairs that conflict with one another access point, while link 7 corresponds to source-destination pairs that conflict with the other two access points, so that no other transmission can occur at the same time.

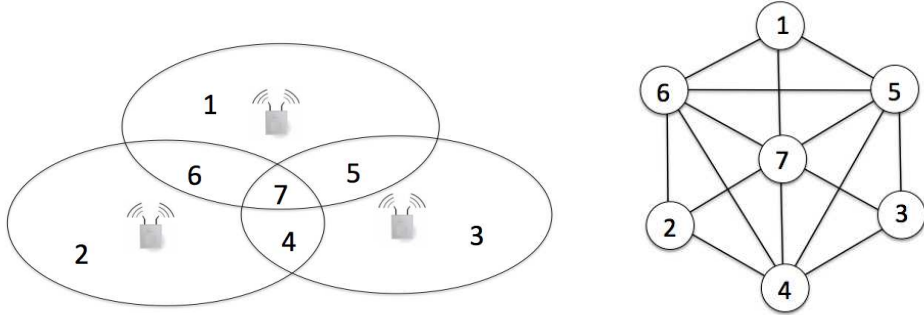


Figure 3: A network of three access points and its conflict graph.

3.2 Capacity region

Let φ_k be the physical rate of link k when scheduled, in bit/s. The throughput of link k when each schedule i is selected with probability p_i , with $\sum_{i=1}^I p_i = 1$, is given by:

$$\forall k = 1, \dots, K, \quad \phi_k = \varphi_k \sum_{j=1}^J \sum_{i: k \in S_{ij}} p_i. \quad (1)$$

Let ϕ be the corresponding throughput vector. We refer to the *capacity region* as the set of vectors ϕ generated by all probability measures p_1, \dots, p_I .

3.3 Flow-level dynamics

Assume that users start file transfers at the times of a Poisson process of intensity $\lambda_k > 0$ at link k . File sizes are assumed to be exponential of mean $\sigma_k > 0$, in bits. Each user leaves the network once the corresponding data transfer, referred to as a flow, is completed. We denote by $\rho_k = \lambda_k \sigma_k$ the traffic intensity at link k (in bit/s) and by ρ the corresponding vector. Let x_k be the number of active users at link k . We refer to the vector x as the network state.

We shall consider random access algorithms that select each schedule i with some probability $p_i(x)$ that depends on the network state x , with $\sum_{i=1}^I p_i(x) = 1$. Under the time-scale separation assumption, the schedules change at a very high frequency compared to the flow-level time-scale, so that the throughput of link k in state x is averaged over all feasible schedules and given by:

$$\phi_k(x) = \varphi_k \sum_{j=1}^J \sum_{i: k \in S_{ij}} p_i(x). \quad (2)$$

The evolution of the network state then defines a Markov process $X(t)$ with transition rates λ_k from state x to state $x + e_k$ and $\mu_k(x) = \phi_k(x)/\sigma_k$ from state x to state $x - e_k$ (provided $x_k > 0$), where e_k denotes the K -dimensional unit vector on component k .

3.4 Stability region

We are interested in the *stability* of the network in the sense of the positive recurrence of the Markov process $X(t)$. This characterizes the maximum traffic intensity the network can sustain. Clearly, a necessary condition is that the vector of traffic intensities ρ lies in the capacity region. We look for distributed access schemes that stabilize the network whenever possible, that is for all vectors of traffic intensities ρ in the interior of the capacity region. The stability region then coincides with the capacity region (up to the boundary) and the corresponding access scheme is referred to as *optimal*.

4 Standard CSMA

4.1 Algorithm

We first consider the standard CSMA algorithm where each transmitter waits for a period of random duration referred to as the *backoff time* before each transmission attempt. At each attempt, the transmitter chooses a radio channel at random and probes it. If the radio channel is sensed idle (in the sense that no conflicting link is active), a packet is transmitted; otherwise, the transmitter waits for a new backoff time before the next attempt.

The source of link k has n_k transmitters and thus can send up to n_k packets at the same time, on distinct channels. Packets have random sizes of mean θ_k bits and are transmitted at the physical rate φ_k ; the backoff times are random with mean τ_k . We denote by $\alpha_k = \theta_k / (\varphi_k \tau_k)$ the ratio of mean packet transmission time to mean backoff time at link k . This may be interpreted as the *attempt rate* of link k , expressed in packet transmission time units. Channel j is chosen with probability β_{kj} , with $\sum_{j=1}^J \beta_{kj} = 1$ and $\beta_{kj} > 0$ if and only if $k \in V_j$, so that each accessible channel is attempted with positive probability.

Remark 1 *Each source may well send a burst of packets instead of a single packet when accessing the channel; the model remains unchanged, with θ_k representing the mean burst size at link k instead of the mean packet size.*

4.2 Associate scheduling

We look for the steady-state probability $p_i(x)$ that the set of active links corresponds to schedule i in state x . By the time-scale separation assumption, the throughput of each link will then follow from (2). We assume that, in state x , each link k such that $x_k > 0$ takes all opportunities offered by the CSMA algorithm to transmit packets; any other link remains idle. If the packet sizes and the backoff times had exponential distributions, the state of each transmitter of link k in isolation would form a Markov process, whose transition graph is given by Fig. 4.

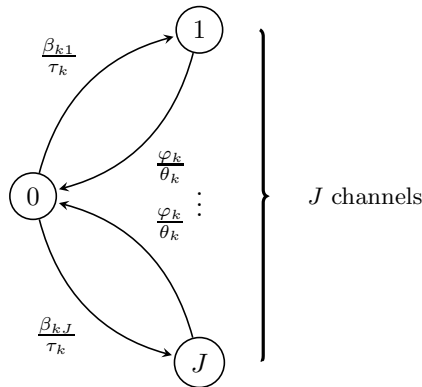


Figure 4: Transition graph of the Markov process describing the state of a transmitter of link k in isolation under standard CSMA.

This Markov process is reversible, with stationary measure equal to 1 for state 0 (transmitter idle) and to $\alpha_k \beta_{kj}$ for state j (transmitter active on channel j), cf. [17]. We deduce that, in the absence of conflicts, the sets of active links S_1, \dots, S_J also form a reversible Markov process, with stationary measure given by 1 if $S_1 = \dots = S_J = \emptyset$ (all transmitters idle) and:

$$\prod_{k: x_k > 0} \binom{n_k}{y_k} \alpha_k^{y_k} \prod_{j: k \in S_j} \beta_{kj}$$

otherwise, where

$$y_k = \sum_{j=1}^J \mathbb{1}(k \in S_j)$$

denotes the number of simultaneous transmissions at link k , with $y_k \leq n_k$. By reversibility, the actual stationary measure induced by the conflict graph is the truncation of this measure to the set of feasible schedules. Specifically, the weight of feasible schedule i in the stationary measure is given by 1 for $i = 1$ (all transmitters idle) and by:

$$w_i(x) = \prod_{k: x_k > 0} \binom{n_k}{y_{ik}} \alpha_k^{y_{ik}} \prod_{j: k \in S_{ij}} \beta_{kj} \quad (3)$$

otherwise, where

$$y_{ik} = \sum_{j=1}^J \mathbb{1}(k \in S_{ij})$$

denotes the number of simultaneous transmissions at link k under schedule i , with $y_{ik} \leq n_k$. By normalizing of the stationary measure, we deduce that schedule i is selected in state x with probability:

$$p_i(x) = \frac{w_i(x)}{\sum_{i'=1}^I w_{i'}(x)}. \quad (4)$$

It turns out that, by the insensitivity property of the underlying loss network [2], this is also the probability that schedule i is selected in state x for *phase-type* distributions of packet sizes and backoff times with the same means; such distributions are known to form a dense subset within the set of all distributions with real, non-negative support [34], so that expressions (3) and (4) are in fact valid for virtually any distributions of packet sizes and backoff times.

4.3 Suboptimality

We now provide simple examples showing the suboptimality of the standard CSMA algorithm. We consider unit physical rates, that is $\varphi_k = 1$ for all links k , and a single transmitter per source, that is $n_k = 1$ for all links k .

We start with a single link, $K = 1$, and a single channel, $J = 1$. The optimal stability condition is $\rho_1 < 1$. In view of (2)-(4), the throughput in state x is given by:

$$\phi_1(x) = \frac{\alpha_1}{1 + \alpha_1}.$$

We deduce the actual stability condition:

$$\rho_1 < \frac{\alpha_1}{1 + \alpha_1}.$$

This loss of efficiency is due to the backoff times, that must be chosen sufficiently small to limit the overhead of the CSMA algorithm. We shall see that the inefficiency of the algorithm persists in the limit of infinitely small backoff times as soon as multiple links compete for access to the radio channel.

Consider the network of Fig. 5 with $K = 3$ links and $J = 1$ channel, further referred to as the *reference network*. We refer to link 2 as the center link and to links 1,3 as the edge links. The optimal stability condition is given by:

$$\rho_1 + \rho_2 < 1 \quad \text{and} \quad \rho_2 + \rho_3 < 1.$$

Assume for simplicity that all links have the same mean packet sizes and the same mean backoff times, so that $\alpha_1 = \alpha_2 = \alpha_3 = \alpha$ for some $\alpha > 0$. Assume also that links 1 and 3 have the same

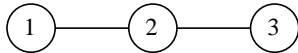


Figure 5: Reference network.

traffic intensities so that $\rho_1 = \rho_3$. The optimal stability condition then reduces to $\rho_1 + \rho_2 < 1$. In view of (2)-(4), the throughputs of links 1 and 2 in state x are given by:

$$\phi_1(x) = \begin{cases} \frac{\alpha}{1+\alpha} & \text{if } x_2 = 0, \\ \frac{\alpha}{1+2\alpha} & \text{if } x_2 > 0, x_3 = 0, \\ \frac{\alpha+\alpha^2}{1+3\alpha+\alpha^2} & \text{if } x_2 > 0, x_3 > 0, \end{cases}$$

and

$$\phi_2(x) = \begin{cases} \frac{\alpha}{1+\alpha} & \text{if } x_1 = 0, x_3 = 0, \\ \frac{\alpha}{1+2\alpha} & \text{if } x_1 > 0, x_3 = 0, \\ & \text{or } x_1 = 0, x_3 > 0, \\ \frac{\alpha}{1+3\alpha+\alpha^2} & \text{if } x_1 > 0, x_3 > 0. \end{cases}$$

The throughput of link 3 follows by symmetry. As for a single link, the backoff times must be chosen sufficiently small to limit the overhead of the algorithm. In the limit $\alpha \rightarrow \infty$ of infinitely small backoff times, we get:

$$\phi(x) = \begin{cases} (1, 0, 1) & \text{if } x_1 > 0, x_3 > 0, \\ (\frac{1}{2}, \frac{1}{2}, 0) & \text{if } x_1 > 0, x_2 > 0, x_3 = 0, \\ (1, 0, 0) & \text{if } x_1 > 0, x_2 = 0, x_3 = 0, \end{cases} \quad (5)$$

the other cases following by symmetry. Note that link 2 is not served when both links 1 and 3 are active. This is due to the fact that link 2 is in conflict with both links 1 and 3 and thus cannot access the channel for null backoff times. This results in a suboptimal stability region:

Proposition 1 *The stability region is given by:*

$$\rho_1 < 1 \text{ and } \rho_2 < \pi_0 + \frac{\pi_{1,3}}{2},$$

where π_0 and $\pi_{1,3}$ are the respective probabilities that both links 1 and 3 are idle and one of the links 1 or 3 is idle, when link 2 is kept active.

The proof is given in the appendix. Note that, when one link is kept active, the other two links form a coupled system of two queues as considered by Fayolle and Iasnogorodski [8], which allows one to calculate π_0 and $\pi_{1,3}$ numerically. Fig. 6 shows that the corresponding stability region is indeed suboptimal. In the homogeneous case $\rho_1 = \rho_2$, the loss of efficiency is around 15%. The inefficiency of the standard CSMA algorithm is thus not only due to the backoff times but to the way the radio channel is allocated between conflicting links.

Finally, we show that standard CSMA algorithm is also suboptimal in the presence of multiple channels. We consider the network of Fig. 7 with $K = 5$ links and $J = 2$ channels, further referred to as the *bow tie network*. The conflict graph is the same for both channels. There is a single transmitter per source, that is $n_k = 1$ for all k . We refer to link 3 as the center link and to the other links as the edge links. As above, we assume that all links have the same mean packet sizes and the same mean backoff times, so that $\alpha_k = \alpha$ for all k , for some $\alpha > 0$. We also assume that all links except link 3 have the same traffic intensities. The optimal stability condition is then given by:

$$\rho_3 < 1 \text{ and } 2\rho_1 + \rho_3 < 2. \quad (6)$$

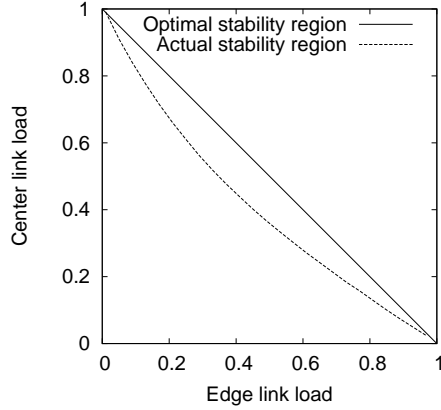


Figure 6: Stability region of the reference network under standard CSMA.

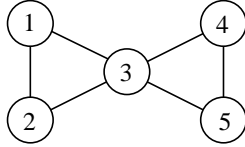


Figure 7: Bow tie network.

Again, we consider the limiting case where $\alpha \rightarrow \infty$. If the two channels are chosen uniformly at random, we deduce from (2)-(4) the following throughput vector:

$$\phi(x) = \begin{cases} (1, 1, 0, 1, 1) & \text{if } x_1, x_2, x_4, x_5 > 0, \\ \left(\frac{3}{4}, \frac{3}{4}, \frac{1}{2}, 1, 0\right) & \text{if } x_1, x_2, x_3, x_4 > 0, \\ & x_5 = 0, \\ \left(\frac{2}{3}, \frac{2}{3}, \frac{2}{3}, 0, 0\right) & \text{if } x_1, x_2, x_3 > 0, \\ & x_4 = x_5 = 0, \\ (0, 1, 1, 1, 0) & \text{if } x_2, x_3, x_4 > 0, \\ & x_1 = x_5 = 0, \\ (1, 1, 0, 0, 0) & \text{if } x_1, x_2 > 0, \\ & x_3 = x_4 = x_5 = 0, \\ (1, 0, 0, 0, 0) & \text{if } x_1 > 0, x_2 = 0, \\ & x_3 = x_4 = x_5 = 0. \end{cases} \quad (7)$$

The other cases follow by symmetry. Again, the center link is in conflict with all other links for accessing the channels and is either not served when all these links are active or served at a low rate when three of them are active. This results also in a suboptimal stability region:

Proposition 2 *The bow tie network is unstable whenever:*

$$\rho_3 > \frac{1}{3}\rho_1^4 - \frac{2}{3}\rho_1^3 - \frac{2}{3}\rho_1^2 + 1. \quad (8)$$

The proof is given in the appendix. In the homogeneous case $\rho_1 = \rho_3$ for instance, Proposition 2 implies that the network is unstable whenever $\rho_1 > 0.63$. In view of (6), the optimal stability

condition is $\rho_1 < 2/3$, which shows that the standard CSMA algorithm is not optimal. This sub-optimality is illustrated by Fig. 8, the actual stability condition being obtained by the simulation of the underlying Markov process. In the homogeneous case for instance, the loss of efficiency is again around 15%.

Remark 2 *Proposition 2 only provides a sufficient condition for instability; this condition is not necessary and thus differs from the actual stability condition, as shown by Fig. 8.*

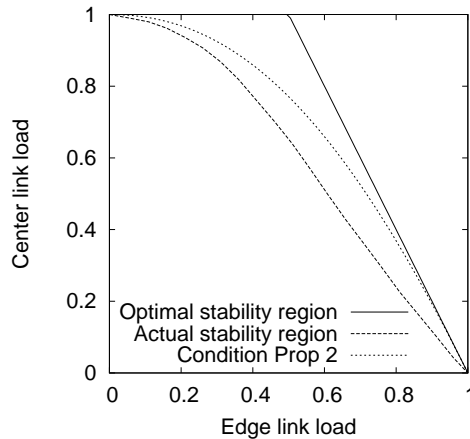


Figure 8: Stability region of the bow-tie network under standard CSMA.

5 User-level CSMA

5.1 Algorithm

We now assume that each transmitter of link k runs x_k independent instances of the CSMA algorithm, one per active user, and sends a packet of the corresponding queue when accessing one of the J channels. Each user then behaves as an independent link, with its own random access scheme.

Remark 3 *The overall attempt rate of each transmitter is proportional to the number of active users at the corresponding MAC interface. Although the results extend to other increasing functions of the number of users, the non-linearity of the function would prevent the algorithm from being implemented through an independent CSMA instance per user. In the example of Fig.3, user-level CSMA is simply achieved by letting each access point run one instance of CSMA per active user, independently of the location of these users in the network and of the corresponding interference constraints.*

Remark 4 *The algorithm gives more frequent access to those links having a large number of active users. Another way to favor these links is to maintain a constant attempt rate and to let each transmitter send one packet per active user when accessing the channel. The algorithm is also optimal but, again, cannot be implemented through a simple CSMA instance per active user.*

We keep the same assumptions and notations as in Section 4. Packets have random sizes of mean θ_k bits and are transmitted at the physical rate φ_k ; the backoff times are random with mean τ_k for each of the x_k flows attempting to access a channel through one of the transmitters of source k . We still denote by $\alpha_k = \theta_k/(\varphi_k\tau_k)$ the corresponding attempt rate expressed in packet transmission time units.

5.2 Equivalent scheduling

We look for the steady-state probability $p_i(x)$ that schedule i is selected in state x . In the absence of conflict, if the packet sizes and the backoff times had exponential distributions, each transmitter of link k would become active after an exponential distribution of mean τ_k/x_k , in any state x such that $x_k > 0$. We deduce that the activity state of this transmitter would form a Markov process, whose transition graph is given by Fig. 9.

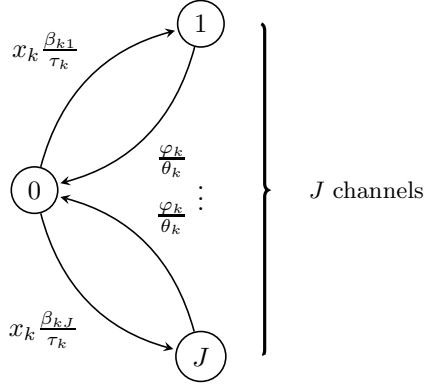


Figure 9: Transition graph of the Markov process describing the state of a transmitter of link k in isolation under user-level CSMA.

This Markov process is reversible, with stationary measure equal to 1 for state 0 (transmitter idle) and to $x_k \alpha_k \beta_{kj}$ for state j (transmitter active on channel j), cf. [17]. We deduce that, in the absence of conflicts, the sets of active links S_1, \dots, S_J on each channel also forms a reversible Markov process, with stationary measure given by 1 if $S_1 = \dots = S_J = \emptyset$ (all transmitters idle) and:

$$\prod_{k: x_k > 0} \binom{n_k}{y_k} (\alpha_k x_k)^{y_k} \prod_{j: k \in S_j} \beta_{kj}$$

otherwise, where

$$y_k = \sum_{j=1}^J \mathbb{1}(k \in S_j)$$

denotes the number of active channels at link k , with $y_k \leq n_k$. By reversibility, the actual stationary measure induced by the conflict graph is the truncation of this measure to the set of feasible schedules. The weight $w_i(x)$ of feasible schedule i in the stationary measure is given by 1 for $i = 1$ (all transmitters idle) and

$$w_i(x) = \prod_{k: x_k > 0} \binom{n_k}{y_{ik}} (\alpha_k x_k)^{y_{ik}} \prod_{j: k \in S_{ij}} \beta_{kj}$$

otherwise, where

$$y_{ik} = \sum_{j=1}^J \mathbb{1}(k \in S_{ij})$$

denotes the number of simultaneous transmissions at link k under schedule i , with $y_{ik} \leq n_k$. Schedule i is then selected with some probability $p_i(x)$ proportional to $w_i(x)$ in state x . By the insensitivity property of the underlying loss network, this probability remains the same for arbitrary phase-type distributions of packet sizes and backoff times with the same means [2].

5.3 Optimality

We now give the main result of the paper, that demonstrates the optimality of the user-level CSMA algorithm.

Theorem 1 *The network is stable for all vectors of traffic intensities ρ in the interior of the capacity region.*

Proof. We apply Foster's criterion. Specifically, we look for some Lyapunov function $F(x)$ such that the corresponding drift, given by:

$$\begin{aligned}\Delta F(x) &= \sum_{k=1}^K \lambda_k (F(x + e_k) - F(x)) \\ &+ \sum_{k:x_k > 0} \mu_k(x) (F(x - e_k) - F(x)),\end{aligned}$$

satisfies:

$$\Delta F(x) \leq -\delta$$

for some $\delta > 0$, in all states x but some finite number.

If the vector of traffic intensities ρ lies in the interior of the capacity region, there exist some $\epsilon > 0$ and some probability measure q_1, \dots, q_I on the set of feasible schedules such that $q_i > 0$ for all $i = 1, \dots, I$ and:

$$\forall k = 1, \dots, K, \quad \rho_k = (1 - 2\epsilon) \varphi_k \sum_{j=1}^J \sum_{i:k \in S_{ij}} q_i. \quad (9)$$

Define:

$$F(x) = \sum_{k:x_k > 0} \frac{\sigma_k}{\varphi_k} x_k \log(\alpha_k x_k).$$

We get:

$$\begin{aligned}\Delta F(x) &= \sum_{k=1}^K \frac{\rho_k}{\varphi_k} (x_k + 1) \log(\alpha_k (x_k + 1)) \\ &- \sum_{k:x_k > 0} \frac{\rho_k}{\varphi_k} x_k \log(\alpha_k x_k) \\ &\quad \sum_{k:x_k > 0} \frac{\phi_k(x)}{\varphi_k} (x_k \log(\alpha_k x_k) \\ &\quad - (x_k - 1) \log(\alpha_k (x_k - 1))),\end{aligned}$$

that is:

$$\begin{aligned}\Delta F(x) &= G(x) + \sum_{k:x_k > 0} \frac{\rho_k}{\varphi_k} (x_k + 1) \log\left(1 + \frac{1}{x_k}\right) \\ &+ \sum_{k:x_k > 0} \frac{\phi_k(x)}{\varphi_k} (x_k - 1) \log\left(1 - \frac{1}{x_k}\right) \\ &+ \sum_{k:x_k = 0} \frac{\rho_k}{\varphi_k} \log(\alpha_k),\end{aligned} \quad (10)$$

with:

$$G(x) = \sum_{k:x_k > 0} \frac{\rho_k - \phi_k(x)}{\varphi_k} \log(\alpha_k x_k).$$

Noting that, for any probability measure p_1, \dots, p_I on the set of feasible schedules:

$$\sum_{k:x_k>0} \sum_{j=1}^J \sum_{i:k \in S_{ij}} p_i \log(\alpha_k x_k) = \sum_{i=1}^I p_i \log(v_i(x)),$$

with:

$$v_i(x) = \prod_{k:x_k>0} (\alpha_k x_k)^{y_{ik}},$$

we get using (2) and (9):

$$\begin{aligned} G(x) &= -\epsilon \sum_{i=1}^I q_i \log(v_i(x)) \\ &\quad + \sum_{i=1}^I (q_i(1-\epsilon) - p_i(x)) \log(v_i(x)). \end{aligned}$$

We then need the following lemma.

Lemma 1 *Let:*

$$v(x) = \max_{i=1, \dots, I} v_i(x).$$

Then, for all states x but some finite number,

$$\sum_{i=1}^I p_i(x) \log(v_i(x)) \geq (1-\epsilon) \log(v(x)).$$

Proof. Let:

$$\mathcal{I}(x) = \left\{ i = 1, \dots, I : \log(v_i(x)) \geq (1 - \frac{\epsilon}{2}) \log(v(x)) \right\}.$$

We have:

$$\sum_{i=1}^I p_i(x) \log(v_i(x)) \geq (1 - \frac{\epsilon}{2}) \log(v(x)) \sum_{i \in \mathcal{I}(x)} p_i(x).$$

Moreover, using the fact that $w_i(x) \leq 2^{KJ} v_i(x)$ for all i and x , we get:

$$\begin{aligned} \sum_{i \notin \mathcal{I}(x)} p_i(x) &= \frac{\sum_{i \notin \mathcal{I}(x)} w_i(x)}{\sum_{i=1}^I w_i(x)}, \\ &\leq 2^{KJ} \frac{\sum_{i \notin \mathcal{I}(x)} v_i(x)}{\sum_{i=1}^I w_i(x)}, \\ &\leq 2^{KJ} \frac{(N - |\mathcal{I}(x)|) v_m(x)^{1-\frac{\epsilon}{2}}}{w_m(x)}, \\ &= 2^{KJ} (N - |\mathcal{I}(x)|) \frac{v_m(x)}{w_m(x)} \frac{1}{v(x)^{\frac{\epsilon}{2}}}, \end{aligned}$$

with:

$$m = \arg \max_{i=1, \dots, I} v_i(x).$$

Since $v(x)$ tends to $+\infty$ when $|x| = \sum_{k=1}^K x_k$ tends to $+\infty$ and the ratio $v_i(x)/w_i(x)$ is bounded for all $i = 1, \dots, I$, this quantity is less than $\epsilon/2$ for all states x but some finite number. We deduce that in all states x but some finite number:

$$\sum_{i=1}^I p_i(x) \log(v_i(x)) \geq (1 - \frac{\epsilon}{2})^2 \log(v(x)) \geq (1 - \epsilon) \log(v(x)).$$

□

In view of Lemma 1, we have for all states x but some finite number:

$$G(x) \leq -\epsilon \sum_{i=1}^I q_i \log(v_i(x)) \\ + (1 - \epsilon) \sum_{i=1}^I (q_i \log(v_i(x)) - \log(v(x))).$$

Since $v_i(x) \leq v(x)$ for all states x , we deduce that for all states x but some finite number:

$$G(x) \leq -\epsilon \sum_{i=1}^I q_i \log(v_i(x)).$$

Since $q_i > 0$ for all $i = 1, \dots, I$, this expression tends to $-\infty$ when $|x| = \sum_{k=1}^K x_k$ tends to $+\infty$. The other terms of $\Delta F(x)$ in (10) being bounded, we deduce that there exists $\delta > 0$ such that $\Delta F(x) \leq -\delta$ for all states x but some finite number. □

6 Simulation Results

This section is devoted to the simulation results. We validate the time-scale separation assumption (packet- vs. flow-level time-scales, cf. §3.3) and compare the throughput performance of standard CSMA and user-level CSMA in various scenarios. We start with the definition of the throughput metric used throughout the section.

6.1 Throughput metric

We evaluate the performance of both algorithms through the *flow throughput*, defined as the ratio of mean flow size to mean flow duration. By Little's law, the flow throughput at link k is given by:

$$\gamma_k = \frac{\rho_k}{\mathbb{E}[x_k]}. \quad (11)$$

Consider the simple case of a single link with a single channel. We have seen that standard CSMA is suboptimal, cf. §4.3. The total throughput is given by:

$$\phi_1 = \varphi_1 \frac{\alpha_1}{1 + \alpha_1},$$

independently of the (positive) number of flows, so that the system corresponds to a processor-sharing queue with arrival rate λ_1 and service rate $\mu_1 = \phi_1/\sigma_1$. In particular, the stability condition is $\rho_1 < \phi_1$ and, under this condition, the steady-state distribution of the number of active users is given by:

$$\pi(x_1) = \left(1 - \frac{\rho_1}{\phi_1}\right) \left(\frac{\rho_1}{\phi_1}\right)^{x_1}.$$

We deduce the mean number of active users:

$$\mathbb{E}[x_1] = \frac{\rho_1}{\phi_1 - \rho_1}$$

and, from (11), the flow throughput:

$$\gamma_1 = \phi_1 - \rho_1.$$

The results are illustrated by Fig. 10 for different values of the attempt rate α_1 , with $\varphi_1 = 1$.

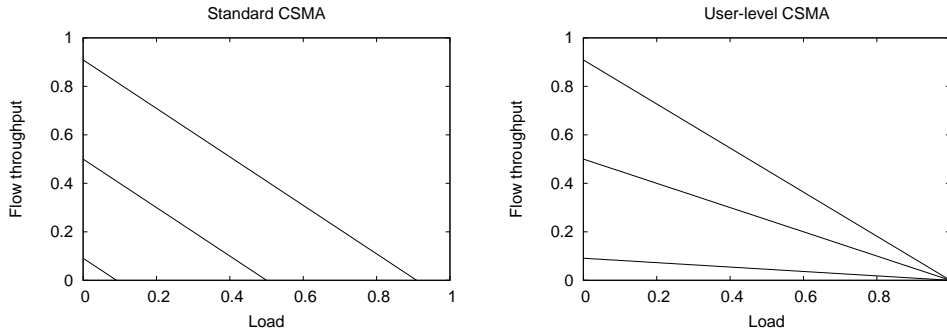


Figure 10: Performance of standard and user-level CSMA for a single link (attempt rate $\alpha_1 = 0.1, 1, 10$, from bottom to top).

Now under user-level CSMA, it follows from (2) that the total throughput of x_1 active users is given by:

$$\phi_1(x_1) = \frac{\alpha_1 x_1}{1 + \alpha_1 x_1}.$$

The system then corresponds to a state-dependent processor-sharing queue with arrival rate λ_1 and service rate $\mu_1(x_1) = \phi_1(x_1)/\sigma_1$. Note that the total throughput $\phi_1(x_1)$ tends to 1 when x_1 tends to infinity. In particular, the stability condition is $\rho_1 < 1$ (which is in fact a consequence of Theorem 1) and, under this condition, the steady-state distribution of the number of active users is given by:

$$\pi(x_1) = \pi(0) \prod_{n=1}^{x_1} \frac{\lambda_1}{\phi_1(n)}.$$

The flow throughput γ_1 then follows from (11). The results are illustrated by Fig. 10 with respect to the load ρ_1 . Note that both algorithms have the same limiting flow throughputs when $\rho_1 \rightarrow 0$, which is simply due to the fact that their behavior is exactly the same in the presence of a single flow. Their performance differs significantly at high loads, due to the suboptimality of the standard CSMA algorithm.

6.2 Time-scale separation assumption

We now assess the validity of the time-scale separation assumption. We consider the reference network of Fig. 2, for which both algorithms differ significantly due to the conflicts suffered by the center link. Unless otherwise specified, we take unit physical rates and unit attempt rates, that is $\varphi_k = 1$ and $\alpha_k = 1$ for all k in the rest of the paper.

Figures 11 and 12 show the flow throughputs under standard CSMA and user-level CSMA, respectively, with and without the time-scale separation assumption. In the former case, we simulate the Markov process $X(t)$, as defined in §3.3; in the latter, we simulate the actual packet-level dynamics, with schedules varying in time depending on the active links and flows consisting of a geometric number of packets with means 20 or 100 packets. In both cases, the flow throughput is estimated from (11) on the basis of 1000 independent simulation runs of 10 millions events, after a warm-up period of 1 million events. Results are shown with respect to the network load $2\rho_1$, in the homogeneous case $\rho_1 = \rho_2 = \rho_3$.

The figures show the 95% confidence intervals of the packet-level simulations. The results suggest that the time-scale separation assumption is valid, even for as low mean flow sizes as 20 packets, so that the properties of standard CSMA and user-level CSMA derived in Sections 4 and 5 under the time-scale separation assumption are likely valid for the actual system. In the rest of this section, we derive the performance of both algorithms from the packet-level dynamics, with a

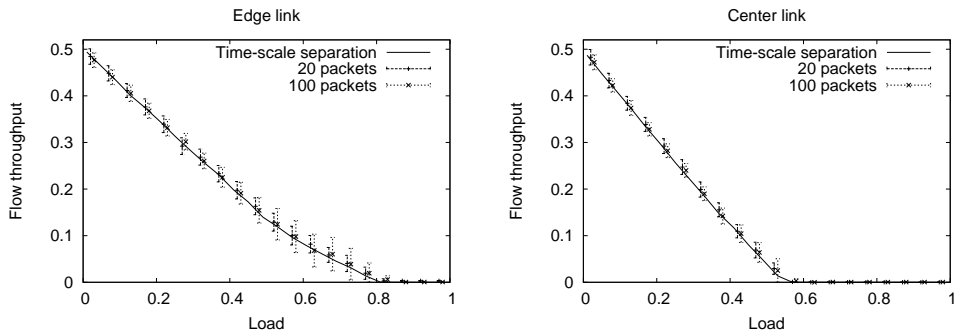


Figure 11: Performance of standard CSMA in the reference network of Fig. 2.

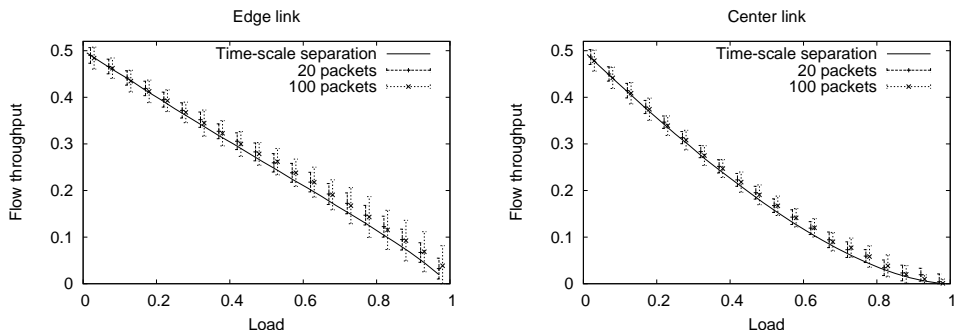


Figure 12: Performance of user-level CSMA in the reference network of Fig. 2.

mean flow size of 100 packets, using the same simulation setting as above; for the sake of clarity, we omit the confidence intervals.

6.3 Number of channels

We first analyze the impact of the number of channels, J . For this purpose, we consider the regular conflict graphs of Fig. 13. In order to simulate a finite number of links and to avoid the border effects, we actually consider the truncated, symmetric, torus versions of these graphs with $K = 16$ edges.

The results are shown in Fig.14 and 15, for $J = 1, 2, 3$ channels, assuming these channels are chosen uniformly at random. Again, we assume homogeneous traffic distributions and show the results with respect to the network load, $2\rho_1$ and $4\rho_1$, respectively. We observe that, while the performance of standard CSMA tends to worsen in the presence of multiple channels, that of user-level CSMA looks approximately insensitive to the number of channels.

6.4 Number of transmitters

Next, we study the impact of the number n of transmitters per link, which is assumed to be the same for all links. The results are shown in Fig.16 and 17, for $J = 3$ channels and $n = 1, 2, 3$ transmitters per link, in the same conditions as above. The flow throughput can be calculated explicitly when the network load tends to 0. It is simply equal to the average number of active transmitters in the presence of a single active user. For an attempt rate of α , we find for $n = 2$:

$$\frac{2\alpha + 4\alpha^2/3}{1 + 2\alpha + 4\alpha^2/3}$$

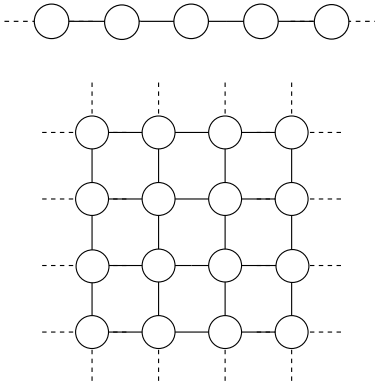


Figure 13: Two regular conflict graphs: line and grid.

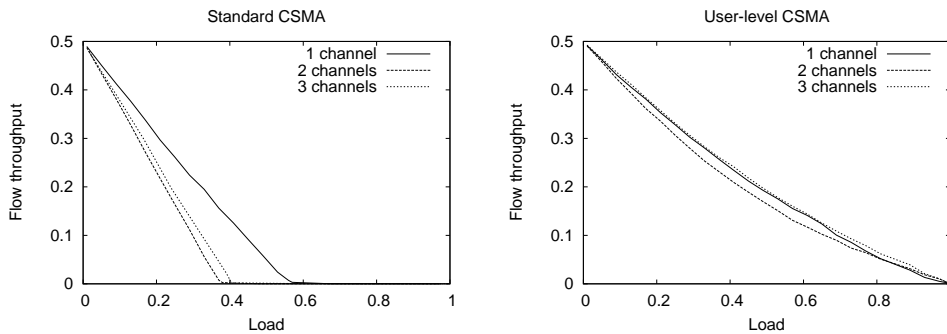


Figure 14: Impact of the number of channels on the performance of standard and user-level CSMA in a line network.

and for $n = 3$:

$$\frac{3\alpha + 4\alpha^2 + 2\alpha^3/3}{1 + 3\alpha + 2\alpha^2 + 2\alpha^3/9}$$

For $\alpha = 1$, we obtain $10/11 \approx 0.9$ and $69/56 \approx 1.2$, respectively, which is compliant with the simulation results of Fig. 16 and 17.

We observe that the performance of standard CSMA tends to improve with the number of transmitters but is still not satisfactory, with a maximum load less than 0.55 in all cases. The user-level CSMA algorithm stabilizes the network independently of the number of transmitters, as long as load is less than 1.

6.5 Network topology

We now study the sensitivity of previous results to the network topology. In addition to the above line and grid topologies, we consider the five conflict graphs depicted by Fig. 18. The random conflict graph is an Erdős-Rényi graph of $K = 20$ nodes and average degree equal to 3. There is a single transmitter per link, and traffic distribution is homogeneous. Table 1 gives for $J = 1$ and $J = 3$ channels, respectively, the maximum loads such that the lowest flow throughput of the network is higher than 0.02 (thus 1 Mbit/s if the common physical rate of all links is equal to 50 Mbit/s). The load is necessarily less than 1, which corresponds to the stability limit where the system becomes unstable. The performance gain of the user-level CSMA algorithm is significant, especially in the presence of multiple channels.

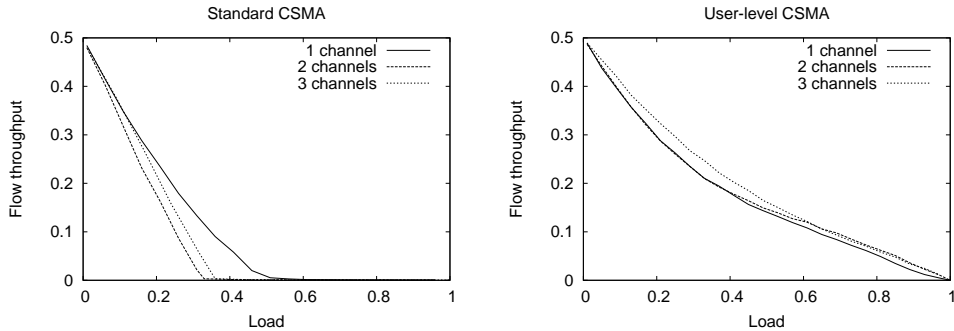


Figure 15: Impact of the number of channels on the performance of standard and user-level CSMA in a grid network.

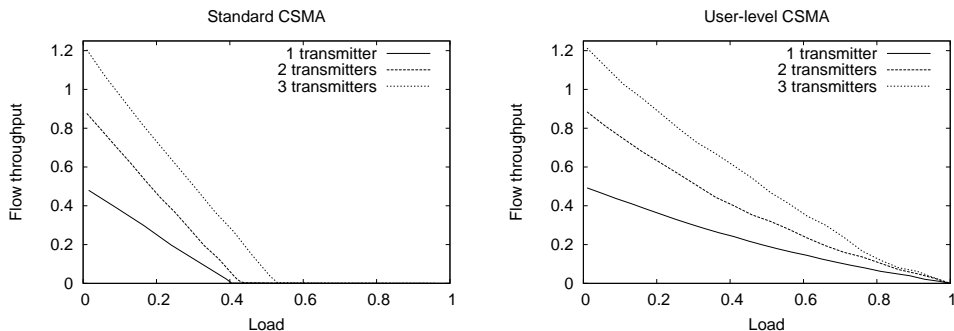


Figure 16: Impact of the number of transmitters on the performance of standard and user-level CSMA in a line network with $J = 3$ channels.

6.6 Channel allocation

Finally, we analyze the behavior of both algorithms when channels are allocated statically so as to avoid interference. In the reference network with $J = 2$ channels for instance, one channel is allocated to the center link and the other channel to the edge links, as illustrated by Fig. 19. The corresponding conflict graphs are $G_1 = (\{2\}, \emptyset)$ and $G_2 = (\{1, 3\}, \emptyset)$ so that there isn't any conflict.

Figure 20 shows the impact of channel allocation on the performance of both algorithms. Of course, the channel allocation reduces the flow throughput at low loads, because there is no scope for reducing interference in this regime whereas each link has access to a single channel instead of two. Surprisingly, it also reduces the flow throughput at high loads under user-level CSMA: the interference avoidance does not compensate for the reduction of available bandwidth. This is not the case of standard CSMA, for which the maximum load slightly increases with channel allocation. These results suggest that, unlike standard CSMA, the dynamic channel allocation achieved by user-level CSMA when links have access to all channels is optimal and that there is no scope for interference avoidance through prior static channel allocation.

7 Conclusion

The distributed scheduling achieved by standard CSMA does not exploit the radio resources in an optimal way. Specifically, the starvation of those links that suffer from high interference may make the network unstable at loads significantly lower than 1. We have proposed a slight modification

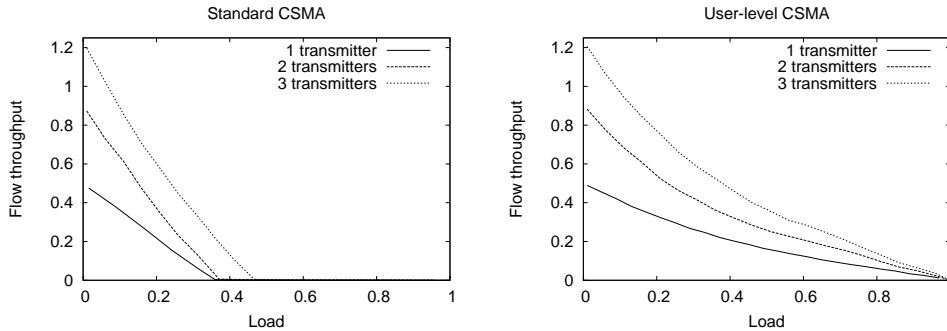


Figure 17: Impact of the number of transmitters on the performance of standard and user-level CSMA in a grid network with $J = 3$ channels.

(a) $J = 1$ channel

Conflict graph	Standard	User-level	Gain
Reference	0.52	0.85	+63%
Line	0.55	0.89	+62%
Grid	0.47	0.90	+91%
Triangle	0.73	0.90	+23%
Star	0.46	0.78	+70%
Hexagon	0.57	0.76	+33%
Random	0.52	0.81	+56%

(b) $J = 3$ channels

Conflict graph	Standard	User-level	Gain
Reference	0.40	0.93	+117%
Line	0.39	0.96	+146%
Grid	0.34	0.96	+182%
Triangle	0.39	0.93	+138%
Star	0.36	0.92	+156%
Hexagon	0.38	0.81	+113%
Random	0.29	0.82	+183%

Table 1: Maximum sustainable load for various network topologies.

of the algorithm whereby each *user* (instead of each link) runs its own CSMA algorithm. This user-level CSMA is provably optimal in the sense that it stabilizes the network whenever possible. Simulation results show that network capacity, in terms of maximum sustainable traffic for some target flow throughput, increases by a factor ranging from 1.5 to 2.5 compared to the standard CSMA algorithm, depending on the network topology and the number of available radio channels.

The analysis relies on a number of simplifying assumptions that we plan to relax in future work. First, we have neglected the impact of packet collisions; these could be included in the model, as done in [13] for rate-based CSMA instance. More generally, the interaction with the standard mechanisms of IEEE 802.11, like the binary exponential back-off scheme, should be studied in details. One may also object that, under user-level CSMA, the attempt rate of a node increases to infinity with the number of users, resulting in high collision rates. Although this point certainly deserves careful attention, we note that the overall attempt rate may also be arbitrarily large under standard CSMA, since there is no limit on the number of users that can connect to some access point and attempt to access the channel. Moreover, the results of §6.1 suggest that the number of active users typically has a geometric tail distribution and thus that the attempt rate is low under user-level CSMA as long as load is not too close to 1. Further analysis is necessary

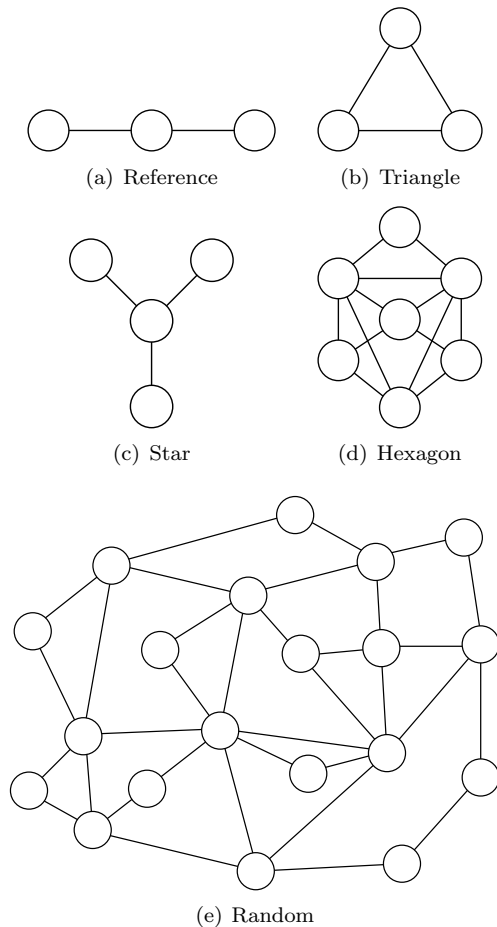


Figure 18: Considered conflict graphs.

to confirm this point.

Other issues that may be worth addressing concern the traffic model. We have only considered elastic traffic, that is typically regulated by the congestion control algorithms of TCP. These are known to strongly impact the performance of IEEE 802.11, due notably to the acknowledgments that must compete for access to the radio channel [27, 18]. The behavior of user-level CSMA in this context is unclear. The impact of non-elastic traffic should also be considered.

From a more theoretical perspective, one may relax the assumption of Poisson flow arrivals and exponential flow sizes in the stability analysis. One may for instance consider user *sessions* that consist of an alternating series of file transfers and idle periods. One may also think of multi-hop networks where the packets of some source-destination pairs must go through one or several relay nodes. Although we believe that user-level CSMA is also optimal in these more general settings, we have not yet been able to prove this result. Moreover, simulations suggest that user-level CSMA is stable without the time-scale separation assumption, which would be worth proving. Finally, it would be interesting to derive bounds or approximations on the throughput performance of both algorithms, so as to confirm the capacity gains obtained in the paper by means of simulation.

Proof of Proposition 1

This example is similar to that considered in [33, p.274]. We analyze the fluid limits of the Markov process $X(t)$. Specifically, we define $X^{(n)}(t)$ as the Markov process $X(t)$ whose initial

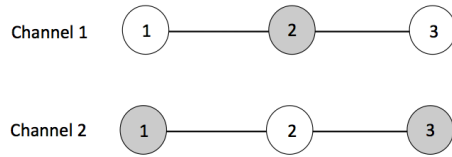


Figure 19: Interference avoidance through channel allocation.

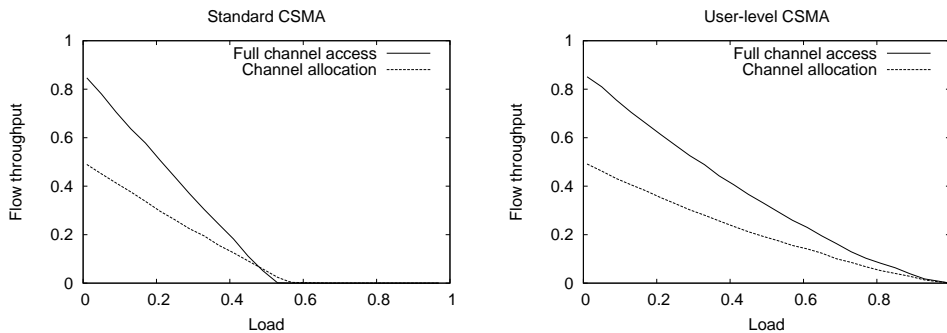


Figure 20: Impact of channel allocation on the performance of standard and user-level CSMA for the center link of the reference network with $J = 2$ channels.

state is $X^{(n)}(0) = (\lfloor \beta_1 n \rfloor, \lfloor \beta_2 n \rfloor, \lfloor \beta_3 n \rfloor)$ for some non-negative real numbers $\beta_1, \beta_2, \beta_3$ such that $\beta_1 + \beta_2 + \beta_3 = 1$. We then define:

$$\bar{X}^{(n)}(t) = \frac{1}{n} X^{(n)}(nt).$$

The fluid limits of the Markov process $X(t)$, if they exist, are the limiting points of this set of processes when $n \rightarrow +\infty$. It is easy to check that the Markov process $X(t)$ belongs to the class (\mathcal{C}) defined in [33, p.241] and that the associated Proposition 9.3 applies. In particular, the set $\{\bar{X}^{(n)}(t), n \in \mathbb{N}\}$ is tight and the fluid limits are continuous. The Markov process $X(t)$ is then positive recurrent if there exists some finite time after which all fluid limits are null, cf. [33, Theorem 9.7]; it is transient if, after some finite time, and for any initial state $\beta_1, \beta_2, \beta_3$, some components of the fluid limits grow at least linearly to infinity [23].

First, note that the three components of the process $X^{(n)}(t)$ behave as three coupled $M/M/1$ queues, with arrival rates $\lambda_1, \lambda_2, \lambda_1$ and state-dependent service rates. We denote by $\mu_k = 1/\sigma_k$ the maximum service rate of queue k , so that $\rho_k = \lambda_k/\mu_k$. As a consequence, if $\rho_k \geq 1$ for some k then $X(t)$ is null recurrent or transient and the network is unstable. In the following, we assume that $\rho_k < 1$ for all k .

We calculate the fluid limit until the first time where one component reaches 0, if any, for all possible initial states. The Markov process is positive recurrent if all queues empty in finite time in the limit and transient if, starting from any initial state, at least one queue grows linearly to infinity after some finite time.

We start with the case $\beta_1 > 0, \beta_2 > 0, \beta_3 > 0$. The three queues are then mutually independent, with respective service rates $\mu_1, 0, \mu_1$. The scaling property of the $M/M/1$ queue shows that the process $\bar{X}^{(n)}(t)$ weakly converges to the function:

$$(\beta_1 + (\lambda_1 - \mu_1)t, \beta_2 + \lambda_2 t, \beta_3 + (\lambda_1 - \mu_1)t),$$

until one of the components 1 or 3 is null.

We now consider the case $\beta_1 = 0$, $\beta_2 > 0$, $\beta_3 > 0$. In view of (5), queue 1 has service rate μ_1 and is empty with probability $1 - \rho_1$. Queues 2 and 3 have service rates 0, μ_1 with probability ρ_1 and $\mu_2/2$, $\mu_1/2$ with probability $1 - \rho_1$. Proposition 9.14 of [33] applies and the process $\bar{X}^{(n)}(t)$ weakly converges to the function:

$$(0, \beta_2 + (\lambda_2 - \mu_2 \frac{1 - \rho_1}{2})t, \beta_3 + \frac{\lambda_1 - \mu_1}{2}t),$$

until one of the components 2 or 3 is null. Since $\rho_1 < 1$, component 3 tends to 0 independently of component 2.

Finally, we consider the case $\beta_1 = \beta_3 = 0$, $\beta_2 > 0$. Note that, in view of the above two cases, components 1 and 3 remain null. The service rate of queue 2 is equal to μ_2 with probability π_0 and to $\mu_2/2$ with probability $\pi_{1,3}$. The process $\bar{X}^{(n)}(t)$ weakly converges to the function:

$$(0, \beta_2 + (\lambda_2 - \mu_2(\pi_0 - \frac{\pi_{1,3}}{2}))t, 0),$$

whenever component 2 is positive. If $\rho_2 < \pi_0 - \pi_{1,3}/2$, component 2 tends to 0 in finite time and $X(t)$ is positive recurrent. If $\rho_2 > \pi_0 - \pi_{1,3}/2$, component 2 increases linearly to infinity and $X(t)$ is transient.

Proof of Proposition 2

Define the throughput vector $\tilde{\phi}$ such that $\tilde{\phi}_3(x) = \phi_3(x)$ and $\tilde{\phi}_k(x) = \mathbb{1}(x_k > 0)$ for all $k \neq 3$. It can be easily verified that $\tilde{\phi}_k(x) \geq \tilde{\phi}_k(y)$ for all states x, y such that $x \leq y$ and all k such that $x_k > 0$. Now consider the coupling of the stochastic processes $X(t)$ and $\bar{X}(t)$ describing the evolution of the queues for the throughputs ϕ and $\tilde{\phi}$, respectively, starting from the same initial state $X(0) = \bar{X}(0)$. It follows from the above monotonicity property that $\bar{X}(t) \leq X(t)$ a.s. at any time $t \geq 0$. In particular, the transience or the null recurrence of $\bar{X}(t)$ implies that of $X(t)$.

For the throughput vector $\tilde{\phi}(t)$, queues 1,2,4,5 are independent $M/M/1$ queues with load ρ_1 . If $\rho_1 \geq 1$, the Markov process $\bar{X}(t)$ is null recurrent or transient. Note that (8) then reduces to $\rho_3 \geq 0$.

Assume now that $\rho_1 < 1$. To prove the transience of $\bar{X}(t)$, we use fluid limits as in the proof of Proposition 1. Since $\rho_1 < 1$ and for $\tilde{\phi}(t)$, queues 1,2,4,5 are independent $M/M/1$ queues with load ρ_1 , there exists some finite time after which, for any initial conditions, the corresponding components of the fluid limit are null. We then just have to consider the fluid limits with the initial condition $\beta_3 = 1$ and $\beta_k = 0$ for $k \neq 3$. In this case, Proposition 9.14 of [33, p.241] applies and the fluid limit satisfies:

$$\bar{X}_3(t) = 1 + (\lambda_3 - \mu_3 \bar{\phi}_3)t,$$

as long as this function is positive, where $\bar{\phi}_3$ is the throughput of link 3 averaged over the states of other links. Since each other link is active with probability ρ_1 , it follows from (7) that:

$$\bar{\phi}_3 = \frac{1}{3}\rho_1^4 - \frac{2}{3}\rho_1^3 - \frac{2}{3}\rho_1^2 + 1.$$

In particular, $\bar{X}_3(t)$ increases linearly to infinity whenever inequality (8) is satisfied and, according to [23], the Markov process $\bar{X}(t)$ is transient.

References

- [1] S. Ben Fredj, T. Bonald, A. Proutière, G. Régnié, and J. W. Roberts. Statistical bandwidth sharing: a study of congestion at flow level. In *Proceedings of ACM SIGCOMM*, pages 111–122, 2001.
- [2] T. Bonald. Insensitive traffic models for communication networks. *Discrete Event Dynamic Systems*, 17(3):405–421, 2007.

- [3] T. Bonald and M. Feuillet. On the stability of flow-aware CSMA. In *IFIP Performance*, 2010.
- [4] T. Bonald, A. Ibrahim, and J. Roberts. Enhanced spatial reuse in multi-cell WLANs. In *IEEE INFOCOM*, 2009.
- [5] T. Bonald and L. Massoulié. Impact of fairness on Internet performance. In *Proceedings of ACM SIGMETRICS/Performance*, pages 82–91, 2001.
- [6] P. Chaporkar, K. Kar, X. Luo, and S. Sarkar. Throughput and fairness guarantees through maximal scheduling in wireless networks. *IEEE Transactions on Information Theory*, 54(2):572–594, feb 2008.
- [7] A. Dimakis and J. Walrand. Sufficient conditions for stability of longest-queue-first scheduling: second-order properties using fluid limits. *Adv. in Appl. Probab.*, 38(2):505–521, 2006.
- [8] G. Fayolle and R. Iasnogorodski. Two coupled processors: The reduction to a riemann-hilbert problem. *Probability Theory and Related Fields*, 47(3):325–351, 1979.
- [9] A. Grilo and M. Nunes. Performance evaluation of IEEE 802.11e. In *International Symposium on Personal, Indoor and Mobile Radio Communications*, volume 1, pages 511–517, 2002.
- [10] A. Gupta, X. Lin, and R. Srikant. Low-complexity distributed scheduling algorithms for wireless networks. *IEEE/ACM Trans. Netw.*, 17(6):1846–1859, 2009.
- [11] L. Jiang, D. Shah, J. Shin, and J. Walrand. Distributed random access algorithm: Scheduling and congestion control. Submitted, 2009.
- [12] L. Jiang and J. Walrand. A distributed CSMA algorithm for throughput and utility maximization in wireless networks. In *the 46th Annual Allerton Conference on Communication, Control, and Computing*, 2008.
- [13] L. Jiang and J. Walrand. Approaching throughput-optimality in a distributed CSMA algorithm: collisions and stability. In *MobiHoc S3'09*, pages 5–8. ACM, 2009.
- [14] L. B. Jiang and S. C. Liew. An adaptive round robin scheduler for head-of-line-blocking problem in wireless LANs. In *IEEE WCNW*, 2005.
- [15] C. Joo, X. Lin, and N. B. Shroff. Understanding the capacity region of the greedy maximal scheduling algorithm in multihop wireless networks. *IEEE/ACM Trans. Netw.*, 17(4):1132–1145, 2009.
- [16] K. Kar, X. Luo, and S. Sarkar. Throughput-optimal scheduling in multichannel access point networks under infrequent channel measurements. *Transactions on Wireless Communications*, 7(7):2619–2629, jul 2008.
- [17] F. Kelly. *Reversibility and Stochastic Networks*. Wiley, Chichester, 1979.
- [18] F. Lebeugle and A. Proutiere. User-level performance in WLAN hotspots. In *ITC 19*, 2005.
- [19] M. Leconte, J. Ni, and R. Srikant. Improved bounds on the throughput efficiency of greedy maximal scheduling in wireless networks. In *MobiHoc'09*, pages 165–174. ACM, 2009.
- [20] S. Liu, L. Ying, and R. Srikant. Scheduling in multichannel wireless networks with flow-level dynamics. In *SIGMETRICS*, 2010.
- [21] S. Liu, L. Ying, and R. Srikant. Throughput-optimal opportunistic scheduling in the presence of flow-level dynamics. In *INFOCOM, 2010 Proceedings IEEE*, pages 1–9, 14-19 2010.
- [22] L. Massoulié and J. W. Roberts. Bandwidth sharing and admission control for elastic traffic. *Telecommunication Systems*, 15:185–201, 2000.

- [23] S. Meyn. Transience of multiclass queueing networks via fluid limit models. *Annals of Applied Probability*, 5:946–957, 1995.
- [24] E. Modiano, D. Shah, and G. Zussman. Maximizing throughput in wireless networks via gossiping. *SIGMETRICS Perform. Eval. Rev.*, 34(1):27–38, 2006.
- [25] M. Neely, E. Modiano, and C. Rohrs. Dynamic power allocation and routing for time-varying wireless networks. *Journal on Selected Areas in Communications*, 23(1):89–103, jan 2005.
- [26] J. Ni, B. Tan, and R. Srikant. Q-CSMA: Queue-length based CSMA/CA algorithms for achieving maximum throughput and low delay in wireless networks. In *IEEE INFOCOM*, 2010.
- [27] S. Pilosof, R. Ramjee, D. Raz, Y. Shavitt, and P. Sinha. Understanding TCP fairness over wireless LAN. In *INFOCOM*, volume 2, pages 863–872, 2003.
- [28] A. Proutière, Y. Yi, and M. Chiang. Throughput of random access without message passing. In *the 46th Annual Allerton Conference on Communication, Control, and Computing*, 2008.
- [29] A. Proutière, Y. Yi, T. Lan, and M. Chiang. Resource allocation over network dynamics without timescale separation. In *IEEE INFOCOM*, 2010.
- [30] D. Qian, D. Zheng, J. Zhang, and N. Shroff. CSMA-based distributed scheduling in multi-hop MIMO networks under SINR model. In *IEEE INFOCOM*, 2010.
- [31] S. Rajagopalan and D. Shah. Distributed algorithm and reversible network. In *CISS*, pages 498–502, 2008.
- [32] S. Rajagopalan, D. Shah, and J. Shin. Network adiabatic theorem: an efficient randomized protocol for contention resolution. In *SIGMETRICS'09*, pages 133–144. ACM, 2009.
- [33] P. Robert. *Stochastic Networks and Queues*. Stochastic Modeling and Applied Probability Series. Springer-Verlag, New York, 2003.
- [34] R. Serfozo. *Introduction to Stochastic Networks*. Springer-Verlag New York, 1999.
- [35] J. So and N. Vaidya. Multi-channel MAC for ad hoc networks: Handling multi-channel hidden terminals using a single transceiver. In *ACM MobiHoc*, pages 222–233, 2004.
- [36] L. Tassiulas and A. Ephremides. Stability properties of constrained queueing systems and scheduling policies for maximum throughput in multihop radio networks. *IEEE Transactions on Automatic Control*, 37:1936–1948, 1992.
- [37] F. Tobagi and L. Kleinrock. Packet switching in radio channels: Part ii—the hidden terminal problem in carrier sense multiple-access and the busy-tone solution. *Communications, IEEE Transactions on*, 23(12):1417–1433, dec 1975.
- [38] A. Tzamaloukas and J. J. Garcia-Luna-Aceves. A receiver-initiated collision-avoidance protocol for multi-channel networks. In *INFOCOM*, pages 189–198, 2001.
- [39] P. van de Ven, S. Borst, and S. Shneer. Instability of MaxWeight scheduling algorithms. In *IEEE INFOCOM*, 2009.
- [40] X. Wu, R. Srikant, and J. R. Perkins. Scheduling efficiency of distributed greedy scheduling algorithms in wireless networks. *IEEE Transactions on Mobile Computing*, 6(6):595–605, 2007.